Magnetic Stars, 2011, pp. 179 – 187

Magnetic Braking of the Main Component of θ^1 Ori C

Balega Yu. Yu.[1], **Leushin V. V.**[1,2], **Weigelt G.**[3]

[1] Special Astrophysical Observatory, Nizhny Arkhyz, Russia
[2] Southern Federal University, Rostov–on–Don, Russia
[3] Max–Planck–Institut für Radioastronomie, Bonn, Germany

Abstract. θ^1 Ori C is the nearest massive O star at the early phase of the evolution. The interferometric study of the star at the 6–m BTA telescope showed that it is a binary system with an orbital period of 11 yr (Weigelt et al., 1999). It was also found that θ^1 Ori C is an oblique magnetic rotator (Donati et al., 2002; Wade et al., 2006). From the high resolution spectra of the binary collected with the 6–m telescope we succeeded to separate weak lines of the secondary component and to measure its rotation velocity. It was found that the secondary rotates three times faster than the primary. We discuss the possibility of magnetic braking of the primary star as the mechanism explaining the difference of rotation.

Key words: stellar magnetic fields – upper main sequence stars – open clusters

1 Introduction

The brightest member of the Orion Trapezium, θ^1 Ori C, is also the most massive star in the group. It is the main source of the ionizing radiation in the centre of the Orion Nebula. Speckle interferometry with the 6–m BTA telescope of the Special Astrophysical Observatory, Russia, showed that it is a close binary system with a rotation period of about 11 years. Orbital parameters of the pair were determined as a result of an 11–year interferometric monitoring campaign (Kraus et al., 2009). Following the orbit, the components of θ^1 Ori C have the following parameters:

component 1	component 2
$T_{\rm eff} = (37000 - 40000\,{\rm K})$	$T_{\rm eff} = (30000 - 33000\,{\rm K})$
$\log L_1/L_\odot = (5.21 - 5.29)$	$\log L_2/L_\odot = (4.68 - 4.76)$
$M_1 = (34.0 - 39.0)\,M_\odot$	$M_2 = (8.0 - 15.5)\,M_\odot$

A large spread of the fundamental parameters is caused by the complexity of atmospheric processes in the system connected with the presence of stellar winds and a gaseous disk around the main component. The analysis is complicated by the presence of a recently discovered magnetic field. In the paper we present the high spectral resolution study of θ^1 Ori C, which was performed to specify the fundamental parameters of the components and to estimate the influence of the magnetic field on the evolution of the star.

2 Observational Data

Table 1 contains the list of the used spectra. Phases refer to the orbital motion of the pair. They were calculated using the elements from Kraus et al. (2009).

Table 1: List of the spectra

Date	Phase	†−⊙	1−⊙	2−⊙	1−†	2−†	Spectral Region	Telescope
3 – 5.03.2000	0.78	−25.0	32	−7	57	18	4500 – 4600	2–m Pic du Midi (Wade et al., 2006)
20.10.2008	0.55	21.5	26	14	5.5	−7.5	3047 – 4525	6–m BTA
17 – 18.12.2008	0.57	−1.9	27	13	29	15	3615 – 9999	2–m Peak Terskol
5 – 6.12.2009	0.655	4.1	28	5	24	1	4397 – 4638	6–m BTA
							4090 – 4335	
27.01.2010	0.666	−18.7	29	2	48	20	4357 – 4598	6–m BTA
27.02.2010	0.674	−25.4	30	2	55	27	4357 – 4598	6–m BTA

Table 2: Parameters of the components

	θ^1 Ori C 1	θ^1 Ori C 2
Mass, $M_\odot$	35.8	10.0
$\log L/L_\odot$	5.20	4.69
Radius, $R/R_\odot$	10.0	8.2
T_{eff}, K	37000	30000
$\log g$	4.01	3.60
Eq. rot. vel., km/s	35.4	96.2
Magn. field, G	500–1500	

For each obtained spectrum we give the radial velocities: of the Earth relative to the Sun (†−⊙), the main component relative to the Sun (1−⊙), the secondary component relative to the Sun (2−⊙), the main component relative to Earth (1 − †), the secondary component relative to Earth (2 − †). The resolution of the BTA spectra is about 40000, the typical signal–to–noise ratio is 2000 per pixel. Interstellar absorption lines of He I 3888, Ca II 3933, 3968, Na I 5890, 5896 and numerous emission lines are observed in the spectra. In addition, practically all hydrogen and helium lines have emission components. Therefore, numerous C, N, O, Ne, Mg, Si, Al and Fe ion absorption lines should be studied in the spectra. They are hardly measurable due to their low intensity.

3 Component Model Atmospheres

At the first step, an analysis of the line spectrum of the components was made using the model atmospheres with the following parameters:

θ^1 Ori C 1: $T_{\rm eff} = 39000$ K, $\log L_1/L_\odot = 5.41$, $M_1 = 34.0\,M_\odot$, $R_1 = 10.7\,R_\odot$, $(\log g)_1 = 3.91$;
θ^1 Ori C 2: $T_{\rm eff} = 31900$ K, $\log L_2/L_\odot = 4.68$, $M_2 = 15.5\,M_\odot$, $R_2 = 7.2\,R_\odot$, $(\log g)_2 = 3.92$.

For these models we have used $V_t = 15$ km/s and the solar chemical composition: H = 1.00, He = 0.089 by mass, $\log N({\rm H}) = 12.00$, $\log N({\rm He}) = 10.95$ by the number of atoms. For other elements the following $\log N$ have been used: C — 8.52, N — 8.01, O — 8.89, Ne — 8.05, Mg — 7.54, Si — 7.51, Fe — 7.63. Model atmospheres were computed using the LLMODELS codes (Shulyak et al., 2004). For these models the synthetic spectra containing absorption lines of the following ions: C II,

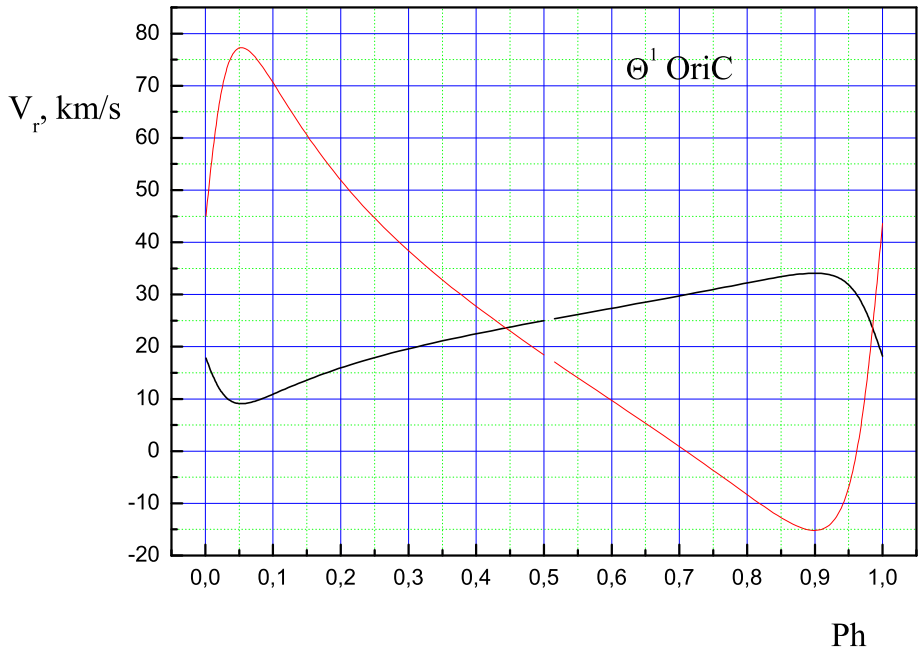

Figure 1: Radial velocities for θ^1 Ori C: thick line corresponds to the velocity of the primary star

C III, C IV, N II, N III, N IV, O II, O III, Ne II, Ne III, Mg II, Si III, Si IV, Al III, and Fe III were calculated with a help of the KONTUR codes (Leushin & Topil'skaya, 1986). A comparison of the synthetic spectra with the observations has shown that the parameters of the components need to be corrected. A similar conclusion arises from the comparison of θ^1 Ori C parameters with the precise masses and radii of stars from the compilation of Torres et al. (2010). After the corresponding corrections, we chose the parameters given in Table 2. They provide the best agreement with the observations, at the same time remaining in the range of values given by the visual orbit (Kraus et al., 2009).

The comparison of fundamental parameters allows to estimate the age of the components: the primary star has just arrived at the main sequence and its age does not exceed 150 000 years, while the secondary is still at the Hayashi stage and moving to the zero age main sequence. Fig. 1 gives the radial velocity curves calculated for the θ^1 Ori C components with the parameters from Table 2 and orbital elements from (Kraus et al., 2009).

4 Rotation Velocities and Absorption Line Profiles in the Spectra of θ^1 Ori C Components

To derive the line profiles in the spectra of the components it is necessary to know their rotation velocities and atmospheric turbulent velocities. Published $v \sin i$ values of the main component θ^1 Ori C1 are spread in a wide range from 24 km/s to 140 km/s (Vitrichenko, 2003; Simon–Dias et al., 2006). From the width of metal absorptions in the spectrum we estimate the rotation velocity $v \sin i = 35$ km/s for the primary star (equatorial rotation velocity is $V_{1\,\mathrm{rot}} = 35.4$ km/s). At the same time, the period of axial rotation of the star is reliably established by Stahl et al. (2008), $P = 15\overset{\mathrm{d}}{.}422$, leading to the equatorial rotation velocity of 33 km/s for the radius $R = 10\,R_\odot$ and

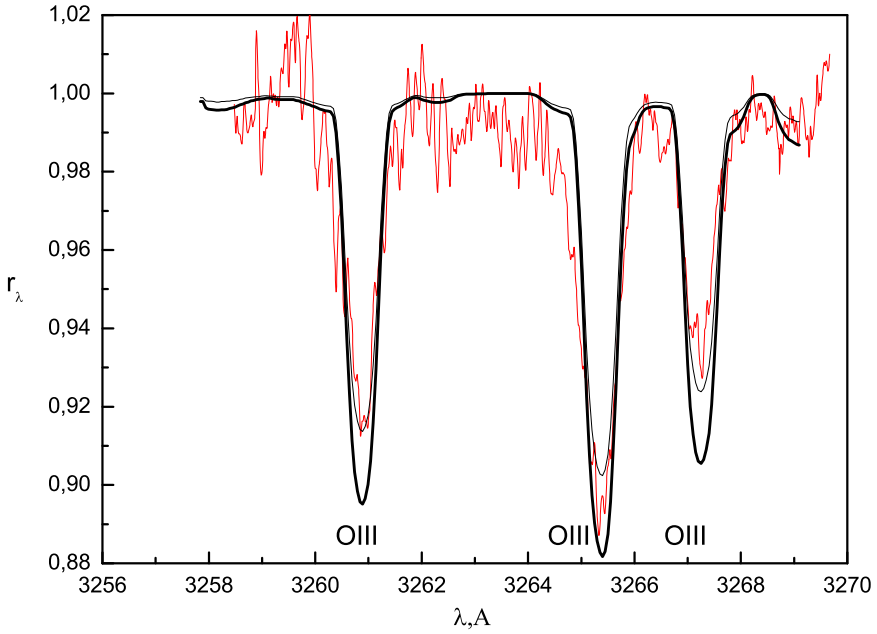

Figure 2: A comparison of the observed part of the spectrum with the synthetic spectrum for the orbital phase 0.55. The thick line corresponds to the chemical composition given in the paper; the thin smoothed line shows the element abundances decreased by 0.3 dex.

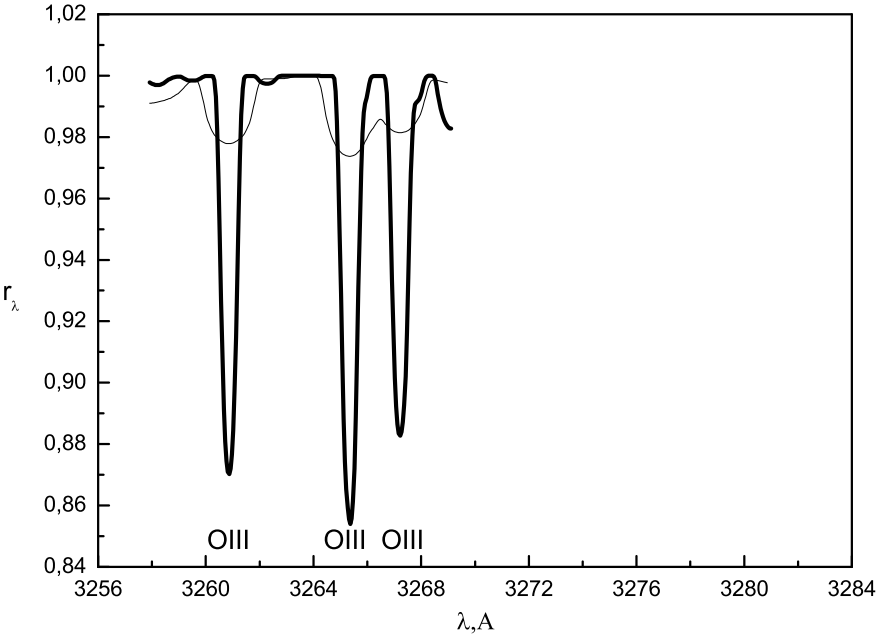

Figure 3: Line profiles for both θ^1 Ori C components: thick line — θ^1 Ori C1 ($v \sin i = 35$ km/s), thin line — θ^1 Ori C2 ($v \sin i = 95$ km/s)

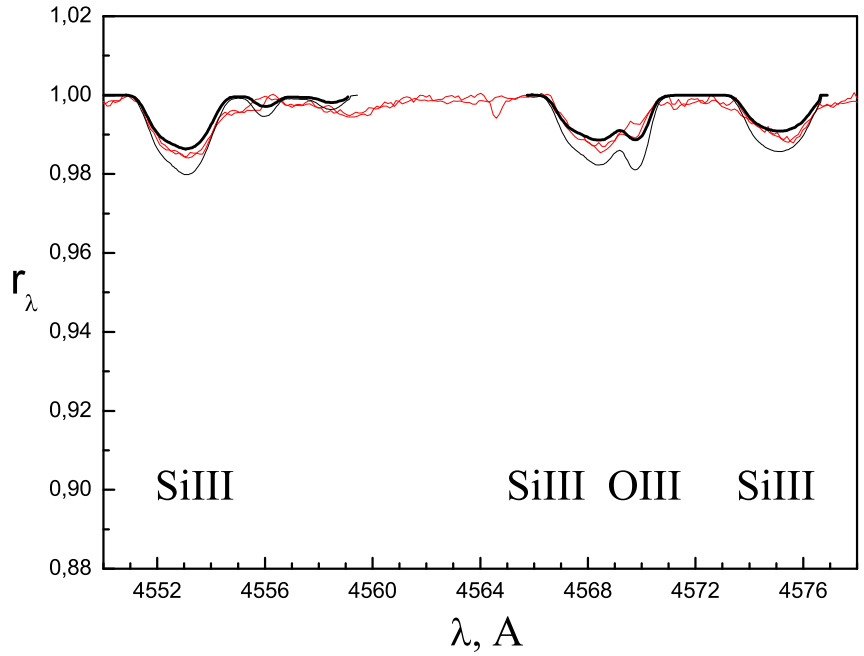

Figure 4: A comparison of the synthetic spectrum with the observed spectra in the region of the Si III triplet for orbital phases 0.666 and 0.674. The thick line corresponds to the chemical composition given in the paper, the thin smoothed line shows the element abundances increased by 0.3 dex.

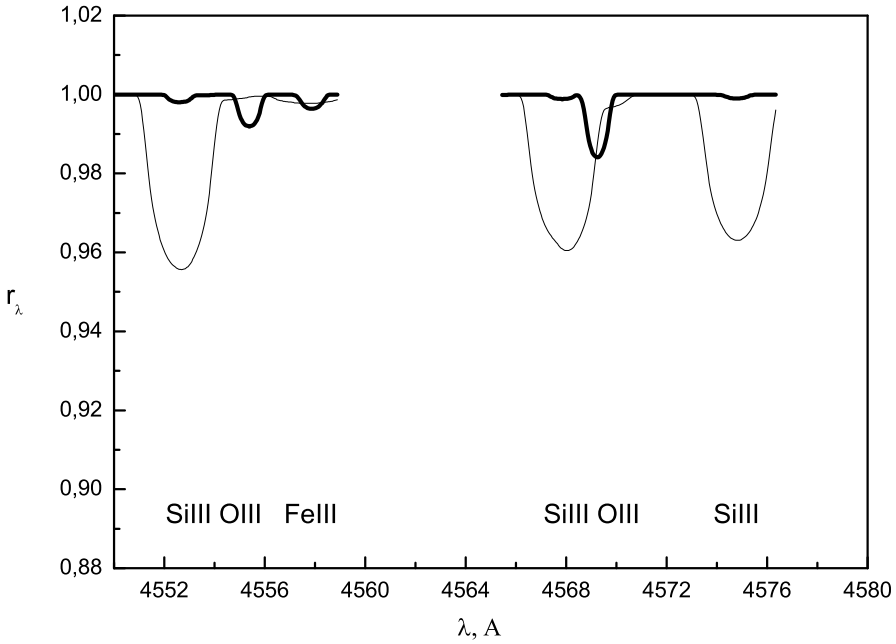

Figure 5: The same as in Fig. 3 for the Si III region.

Table 3: Line parameters for the synthetic spectrum calculation

Ion	λ, Å	ε_i, eV	$\log gf$	Ion	λ, Å	ε_i, eV	$\log gf$
O III 3261 – 3267 Å							
C III	3258.01	38.36	−2.108	**O III**	**3265.32**	**36.47**	**0.432**
He I	3258.27	20.61	−2.508	O III	3265.68	43.41	−0.810
C III	3259.50	38.36	−1.631	**O III**	**3267.20**	**36.43**	**0.101**
O III	**3260.85**	**36.45**	**0.272**	O III	3267.72	43.41	−0.936
C III	3262.26	38.36	−1.409	O III	3268.94	43.41	−0.714
Si III 4553 – 4575 Å							
Fe III	4548.99	20.88	−1.66	Ne I	4565.55	34.82	1.59
N II	4552.94	23.48	0.33	V III	4567.59	20.18	0.95
Si III	**4552.62**	**19.02**	**0.18**	**Si III**	**4567.84**	**19.02**	−0.04
Ca III	4553.29	45.06	0.05	Ne II	4569.06	34.93	0.14
Ne II	4553.40	34.83	−0.80	O III	4569.26	45.99	0.07
Si III	**4554.00**	**28.12**	−0.16	Ne II	4574.42	34.84	−1.16
O III	4555.38	46.92	−0.41	**Si III**	**4574.76**	**19.02**	−0.51
O II	4557.73	31.37	−0.32	V III	4574.92	20.18	−0.27
O II	4557.91	46.92	−0.89	Ne II	4575.72	36.18	−1.64
Fe III	4558.85	55.11	−0.53	Ne II	4576.32	37.48	−1.71

to $v \sin i = 32$ km/s for $i = 105°$. The rotation velocity of the secondary has never been defined before. The principal problem is to select the absorption lines of the secondary in the integral spectrum of θ^1 Ori C. Most of absorptions are formed in the atmosphere of the main star, but the secondary can also contribute noticeably to the line profiles. Figure 2 gives an example of comparison of the calculated O III line profiles with the observed spectrum for the orbital phase 0.55. For this phase, $V_{r\,1} = 26$ km/s and $V_{r\,2} = 14$ km/s relative to the Sun, and $V_{r\,1} = 5.5$ km/s, $V_{r\,2} = -7.5$ km/s relative to Earth. To calculate the line profiles the following turbulent and rotation velocities were accepted: $V_{\rm turb\,1} = 5$ km/s, $(v \sin i)_1 = 35$ km/s, for the main component, and $V_{\rm turb\,2} = 10$ km/s, $(v \sin i)_2 = 95$ km/s, for the secondary. The accepted parameters correspond to the observed line profiles.

Figure 3 shows the profiles of these lines for each component separately. It can be seen that the profile is defined by the main component. Magnitude difference between the components, $L_2/L_1 = 0.3$ (Kraus et al., 2009), must be considered when summing the spectra. Thus, the width of the analyzed lines is defined by the rotation velocity of the main component and corresponds to $(v \sin i)_1 = 35$ km/s. A comparison of the observed and calculated profiles for the Si III triplet spectral region is presented in the same scale in Fig. 4. Figure 5 shows the profiles of these lines separately for each of the components. From this figure it follows that the Si III triplet lines in the summed spectrum of θ^1 Ori C belong to the secondary component and their width reflects its rotation velocity.

The secondary rotates with a significantly higher velocity than the primary star. The averaged spectrum obtained with the BTA 6–m telescope at different phase of orbital period gives the width of Si III triplet lines at half maximum of $\Delta\lambda = 5.10$, 4.62 and 4.27Å, leading to the rotation velocity of the secondary $(v \sin i)_2 = 146.9$ km/s. The width of the lines can be increased by other effects, so we accept $(v \sin i)_2 = 95$ km/s as the lower limit of rotation of the secondary. Further on, we used this velocity to calculate the profiles of other lines. Table 3 gives the parameters of lines, which were used for synthetic spectrum calculations.

Fig. 6 can serve as an additional confirmation of the Si III triplet formation in the atmosphere of

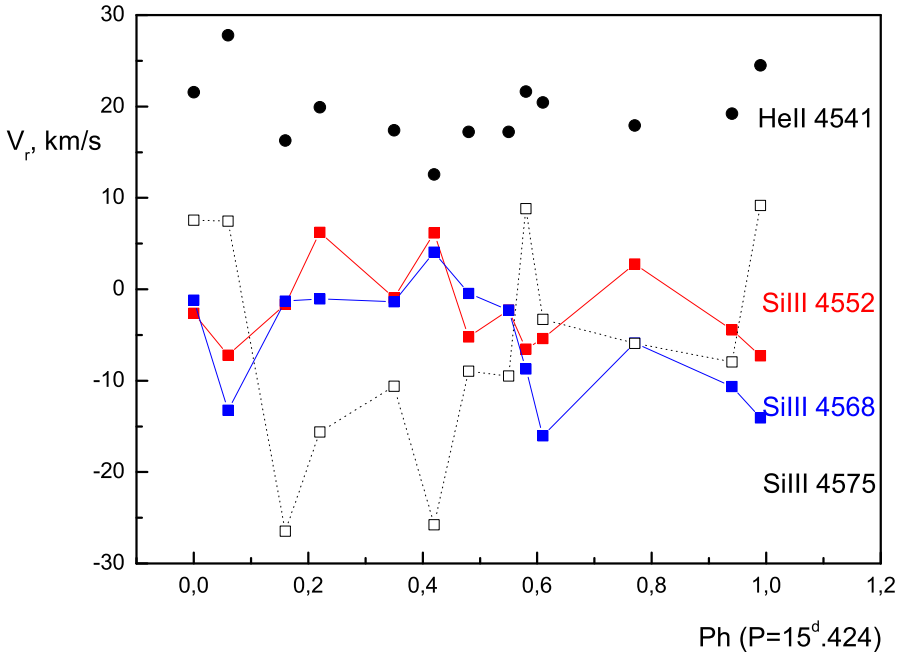

Figure 6: Radial velocities of the components measured from He II and Si III lines for the orbital phase 0.78 relative to the phase of rotation of the primary component (Stahl et al., 2008).

the secondary component. It shows radial velocity measurements for the He II lines formed in the atmosphere of the primary component and for the Si III lines $\lambda\lambda$ 4552.62, 4567.84 and 4574.76 Å. We used the spectra from (Wade et al., 2006) to estimate the radial velocities of the components for the orbital phase 0.78. The primary component's He II He II 4541 "stable" lines were compared with the Si III triplet lines $\lambda\lambda$ 4552.62, 4567.84, 4574.76 Å. Our orbit gives radial velocities $V_{r\,1} = +32$ km/s and $V_{r\,2} = -7$ km/s for this phase, which is in good agreement with the observations. Here we used the published data from (Wade et al., 2006) for the phase Ph = 0.78 which corresponds to our radial velocities $V_{r\,1} = 32$ km/s and $V_{r\,2} = -7$ km/s. All the data evidently show a significant difference in the rotation velocities of the two components.

5 Magnetic Braking

Both components of the binary were formed as a result of fragmentation of a non–magnetic (or weakly magnetic) cloud. We assume that the secondary star θ^1 Ori C2 has a constant rotation velocity $V_{\mathrm{rot}\,2}$. We also assume that the initial rotation of the primary star θ^1 Ori C1 was similar to the rotation of θ^1 Ori C2. Then, the initial rotation velocity of θ^1 Ori C1 was

$$V^0_{\mathrm{rot}\,1} = \frac{R_1}{R_2} V^0_{\mathrm{rot}\,2} = \frac{10.70}{7.94} \cdot 96.2 = 130\,\mathrm{km/s}.$$

Note that the components of all well–studied detached O to early B–type stars show rotation velocities in the range of 100 – 200 km/s (Torres et al., 2010). The original rotation energy of θ^1 Ori C1 was

$$E^0_{\mathrm{rot}\,1} = 2,61 \cdot 10^{48}\,\mathrm{erg}.$$

Then, for the age of 150 000 yrs and the total luminosity of the star $7.5 \cdot 10^{38}$ erg/s, the rate of the energy dissipation is $0.5 \cdot 10^{36}$ erg/s. A strong dipolar magnetic field was first detected on the surface of θ^1 Ori C through the spectropolarimetric observations by Donati et al. (2002). Let us consider magnetic braking as a possible explanation for the slow rotation velocity of the primary. An upper estimate for the magnetic energy of θ^1 Ori C1 is:

$$E_{\rm magn\,1} = B_0^2/8\pi \cdot 4/3\pi R_1^3 = 1.7 \cdot 10^{40} \div 2.7 \cdot 10^{41}\,{\rm erg},$$

where B_0 is the dipolar component of the surface magnetic field. Magnetic energy of the star is a very small part of its rotational energy

$$E_{\rm rot\,1} = 0.2 M_1 \Omega_1^2 R_1^2 = 2 \cdot 10^{47}\,{\rm erg},$$

where $\Omega_1 = 2\pi/P_1$.

Magnetic braking due to the angular momentum carried away by the electromagnetic radiation from the rotating magnetic field gives the following period change (Longair, 1994):

$$\frac{\dot{P}}{P} = \frac{8\pi^2 R^4 B_0^2}{3\kappa c^3 M P^2},$$

where κ is a dimensionless constant, $\kappa = 0.05 - 0.1$ for our mass range. For θ^1 Ori C1 parameters with $B_0 = 1 - 1.5$ kG (Wade et al., 2006), it gives $\dot{P}/P \sim 2 \cdot 10^{-13}\,{\rm yr}^{-1}$. We see that the spin–down time in this case is seven orders of magnitude smaller than needed for the life–time of θ^1 Ori C1.

In the study of the magnetic properties of θ^1 Ori C1, Donati et al. (2002) and Wade et al. (2006) used the Babel & Montmerle (1997) model, in which the magnetic field confines the stellar wind from the magnetic hemispheres towards the magnetic equatorial plane to explain the wide set of spectroscopic observations of the star. From these results it follows that the magnetically confined stellar wind could be the reason for the spin–down of the main star. The angular momentum dissipation for a simple monopole magnetic field is (Weber & Davis, 1967):

$$J = \frac{2}{3}\dot{M}\Omega R_A^2,$$

here $\dot{M}$ is the mass loss rate and R_A is a characteristic Alfven radius. Ud–Doula et al. (2009) modified the momentum loss equation for the case of dipolar magnetic field:

$$\dot{J} = \frac{2}{3}\dot{M}\Omega R^2 [0.29 + (\eta + 0.25)^{1/4}]^2,$$

where η is the wind confining parameter ($\eta = B^2R^2/MV_\infty$). In the case of dipole field the spin–down time scales slower than for a monopole field.

Spin–down time for a magnetic dipole star in the strong–confinement limit is:

$$\tau_{\rm spin} = J/\dot{J} = \frac{3/2\varepsilon M}{BR}\sqrt{\frac{V_\infty}{M}},$$

with typically $\varepsilon \approx 0.1$.

For the θ^1 Ori C1 parameters derived above, we obtain the spin–down time of $\tau_{\rm spin} = 10$ Myr for the moderate magnetic confinement, $\eta = 30$, mass–loss rate $\dot{M} = 4 \cdot 10^{-7}\,M_0/{\rm yr}$ and the wind terminal speed of 2500 km/s (Donati et al., 2006). This value is two orders of magnitude higher than needed to explain the magnetic braking of θ^1 Ori C1. However, even a moderate rate of mass loss leads to a disproportionately large rate of the angular momentum loss (Mestel, 1999). A significantly higher mass loss rate could exist at the early evolution phase of the star. Other examples of hot

stars with fast magnetic braking are HD 191612 with $P = 538$ d (Donati et al., 2006), and HD 108 (Martins et al., 2010). The spin–down time for HD 191612 is only 0.4 Myr, however, its estimated mass loss is higher than for θ^1 Ori C1 ($\dot{M} = 6 \cdot 10^{-6}\, M_0/\mathrm{yr}$). HD 108 might be an extreme case of the slowly rotating magnetic O star. With $\dot{M}$, B, η and V_∞ values similar to θ^1 Ori C1, its rotation velocity is lower than 0.1 km/s. Future observations will show whether the angular momentum loss due to magnetic braking is effective enough to explain the slow rotation velocities of these stars.

6 Summary

On the basis of high–resolution, high signal–to–noise ratio spectra of θ^1 Ori C collected mainly with the 6–m BTA telescope, we have shown that the rotation velocities of the two components are significantly different: the secondary star rotates three times faster than the primary magnetic star. We suppose that the magnetic field of the more massive primary component of θ^1 Ori C could cause its fast magnetic braking. Contrary to that, the fast rotation of the secondary star in the system is explained by the absence of magnetic field. The difference of physical parameters of the components can explain why the primary star generates the field, while the secondary does not. At the same time, the fact that only one star in the binary system possesses a magnetic field could be an indirect evidence of the non–relic nature of stellar magnetic fields. We suppose that the effective magnetic braking happened at the very early main sequence evolutionary stages of the star, when the mass loss was higher than at the present stage. The mass loss rate of θ^1 Ori C1 is poorly constrained. Therefore, it is difficult to reach a satisfactory accordance between the magnetic braking theory and the observed parameters of the star.

References

Babel J., Montmerle T., 1997, A&A, 323, 121
Donati J.–F., Babel J., Harries T. J., Howarth I. D.; Petit P., Semel M., 2002, MNRAS, 333, 55
Donati J.–F., Howarth I. D., Bouret J.–C., Petit P., Catala C., Landstreet J., 2006, MNRAS, 365, L6
Kraus S., Weigelt G., Balega Yu. Yu., Docobo J. A., Hofmann K.–H., Preibisch T., Schertl D., Tamazian V. S., Driebe T., Ohnaka K., Petrov R., Schöller M., Smith M., 2009, A&A, 497, 195
Leushin V. V., Topilskaya G. P., 1986, Astrophysics, 25, 415
Longair M.S., 1994, High energy astrophysics, Vol. 2, "Stars, the Galaxy and the Interstellar Medium", Cambridge Univ. Press, Cambridge (UK)
Martins F., Donati J.–F., Marcolino W. L. F., Bouret J.–C., Wade G. A., Escolano C., Howarth I. D., 2010, MNRAS, 407, 1423
Mestel L., 1999, "Stellar Magnetism", Oxford Univ. Press
Shulyak D., Tsymbal V., Ryabchikova T., Stütz Ch., Weiss W. W., 2004, A&A, 428, 993
Simon–Dias S., Herrero A., Esteben C., Najarro F., 2006, A&A, 448, 351
Stahl O., Wade G., Petit V., Stober B., Schanne L., 2008, A&A, 487, 323
Torres G., Andersen J., Gimenez A., 2010, Astron. Astroph. Rev, 18, 67
Ud–Doula A., Owocki S. P., Townsend H. D., 2009, MNRAS, 392, 1022
Vitrichenko E.A., 2003, "Orion Trapezium", Moscow
Wade G.A., Fullerton A.W., Donati J.–F., Landstreet J. D., Petit P., Strasser S., 2006, A&A, 451, 195
Weber E. J., Davis L. J., 1967, ApJ, 148, 217
Weigelt G., Balega Yu., Preibisch Th., Schertl D., Schöller M., Zinnecker H., 1999, A&A, 347, L15